Disruption of *mRad50* causes embryonic stem cell lethality, abnormal embryonic development, and sensitivity to ionizing radiation

GUANGBIN LUO*†, MICHELLE S. YAO†‡, CARLA F. BENDER§, MICHAEL MILLS*, ANTHONY R. BLADL§, ALLAN BRADLEY*¶, AND JOHN H. J. PETRINI§∥

*Department of Molecular and Human Genetics and ¶Howard Hughes Medical Institute, Baylor College of Medicine, Houston, TX 77030; and ‡Department of Radiation Oncology and §Laboratory of Genetics, University of Wisconsin Medical School, Madison, WI 53706

Communicated by Paul Ahlquist, University of Wisconsin, Madison, WI, April 29, 1999 (received for review February 19, 1999)

ABSTRACT   The Mre11/Rad50 protein complex functions in diverse aspects of the cellular response to double-strand breaks (DSBs), including the detection of DNA damage, the activation of cell cycle checkpoints, and DSB repair. Whereas genetic analyses in *Saccharomyces cerevisiae* have provided insight regarding DSB repair functions of this highly conserved complex, the implication of the human complex in Nijmegen breakage syndrome reveals its role in cell cycle checkpoint functions. We established *mRad50* mutant mice to examine the role of the mammalian Mre11/Rad50 protein complex in the DNA damage response. Early embryonic cells deficient in *mRad50* are hypersensitive to ionizing radiation, consistent with a role for this complex in the repair of ionizing radiation-induced DSBs. However, the null *mrad50* mutation is lethal in cultured embryonic stem cells and in early developing embryos, indicating that the mammalian Mre11/Rad50 protein complex mediates functions in normally growing cells that are essential for viability.

DNA damage is induced by extrinsic agents such as ionizing radiation and also arises spontaneously as an outcome of cellular processes such as DNA replication and oxidative metabolism. The cellular response to DNA damage involves the integration of pathways that detect and signal the presence of DNA damage, activate DNA damage-dependent cell cycle checkpoints, and mediate DNA repair. Genetic defects that impair any of these aspects of the cellular DNA damage response invariably lead to genomic instability. Studies in *Saccharomyces cerevisiae* and human cells have shown that the Mre11/Rad50 protein complex functions in DNA damage detection and signaling as well as in the repair of DNA double-strand breaks (DSBs) (1–3). Hence, this highly conserved protein complex appears to play a central role in the cellular response to DSBs, linking DSB repair to cell cycle checkpoint functions.

Genetic analyses indicate that in mitotic cells, the *S. cerevisiae* Mre11/Rad50 protein complex functions in the repair of chromosomal DSBs through nonhomologous end joining (4–7). Mutations affecting the *S. cerevisiae* complex also lead to genomic instability in the form of increased chromosome loss and spontaneous loss of heterozygosity (i.e., allelic recombination) (2). In meiosis, the *S. cerevisiae* Mre11/Rad50/Xrs2 protein complex is critical to the initiation of meiotic recombination (8). In addition to these roles in DNA recombination and repair, recent data suggest that the *S. cerevisiae* Mre11/Rad50 protein complex also is linked to regulatory functions in the yeast cellular DNA damage response. Mutations in *ScMRE11* suppress the inability of *Yku70* mutants to overcome

DSB-induced cell cycle arrest (9). Further, the response of *Scrad50* mutants to hydroxyurea treatment suggests that the yeast Mre11/Rad50 complex also may function in the activation of the S phase cell cycle checkpoint (10).

Two recent observations link the human Mre11/Rad50 complex to DSB recognition and the activation of cell cycle checkpoints. First, hMre11 localizes to DSBs after ionizing radiation exposure, remaining associated until repair is complete (11). Second, null mutations of p95, a third member of the human Mre11/Rad50 complex, cause Nijmegen breakage syndrome, a chromosomal instability disorder associated with cell cycle checkpoint defects. Although Nijmegen breakage syndrome cells do not appear to be grossly DSB repair-deficient (12), *in vitro* data support the hypothesis that the human complex plays a direct role in DSB repair (13). To define the *in vivo* functions of the murine Mre11/Rad50 protein complex, we mutated *mRad50* in embryonic stem (ES) cells and explored the consequences of this mutation in mice. The null *mrad50* mutation is lethal in cultured ES cells and in early developing embryos. Although early embryonic cells will proliferate in the absence of mRad50, they are hypersensitive to ionizing radiation. These data indicate that whereas the DSB recognition and signaling functions of the Mre11/Rad50 complex are dispensable (14, 15), these proteins mediate other functions that are essential for cell viability.

METHODS

Plasmid Vector Construction. Two targeting vectors, *pTV1* and *pTV2*, were constructed by using 9.4 kb of *mRad50* genomic sequence, isolated from a murine 129/Sv genomic library (Fig. 1*a*). To construct *pTV1*, a 1-kb *Sma*I/*Eco*RV fragment containing exon 1 was replaced by a *PGK-neo* (16) cassette, generating a replacement vector with a total of 8.4 kb of homology (3.8 kb of 5′ homology and 4.6 kb of 3′ homology). In *pTV2*, a *loxP* site from *pBS246* (GIBCO/BRL) was introduced into intron 2, and a *PGK-neo-HSVtk* cassette flanked by a pair of *loxP* sites was inserted upstream of exon 1. The modifications in *pTV2*, when introduced into the *mRad50* locus to create a conditional null allele, do not disrupt the expression of the *mRad50* gene. Both *TV1* and *TV2* include a silent T → A mutation at coding nucleotide 162 in exon 2 that creates a novel *Bsr*GI restriction enzyme-recognition site, allowing discrimination between transcripts from endogenous and targeted alleles. The *mRad50* expression construct, *pmRad50*, was constructed by the insertion of the full-length

PNAS is available online at www.pnas.org.

Abbreviations: DSB, double-strand break; ES, embryonic stem; E, embryonic day.
†G.L. and M.S.Y. contributed equally to this work.
∥To whom reprint requests should be addressed at: Laboratory of Genetics, University of Wisconsin Medical School, 445 Henry Mall, Genetics Building, Madison, WI 53706. e-mail: jpetrini@facstaff.wisc.edu.

cDNA of the *mRad50* gene into the *Nco*I/*Nde*I vector fragment of *pPGKHL231pA* (17), placing *mRad50* expression under the control of a *PGK* promoter. The Cre recombinase expression vector *pOG231* and the *PGK-puropA* construct have been described (18).

Generation and Identification of Mutant ES Cells and Mice. ES cells were cultured on SNL76/7 feeder layers (19). Transfections, drug selection, clonal expansion on 96-well plates, screening, and generation of chimeras were performed by using published procedures (20). Southern blot hybridization analysis was used to identify the targeted allele both in the ES cells and in mice by using established methods. AB2.2 ES cells were electroporated with the targeting vectors *pTV1* or *pTV2*. Targeted ES cell clones were identified by Southern blot hybridization by using the same strategy detailed in Fig. 1. Specifically, targeted clones first were identified by using a 5′ external probe (5P) and then confirmed by using a 3′ external probe (3P). The targeted allele derived from the *pTV1* vector was designated *mrad50*Brdm1, whereas the targeted allele derived from *pTV2* was designated *mrad50*Brdc1. To convert the *mrad50*Brdc1 allele into a null allele, ES cells containing the conditional null allele were electroporated with the *pOG231* Cre expression plasmid and plated at a low density (500 cells per 10-cm plate). 1-(2-Deoxy-2-fluoro-β-D-arabinofuranosyl)-5-iodouracil (FIAU)-resistant colonies were selected and analyzed by Southern blot hybridization as illustrated in Fig. 1. The mutant allele with both the *PGK-neo/HSVtk* cassette and exons 1 and 2 of the *mRad50* gene removed was designated *mrad50*Brdm2. To convert the *m2/c1* genotype into *m2/m2*,

supercoiled *pOG231* was co-electroporated with linearized *pmRad50* and *PGK-puropA* followed by FIAU–puromycin double selection.

Immunologic Analyses. Immunoprecipitations with preimmune serum or mMre11 antiserum and protein analysis by immunoblot were as described (21), using mRad50 mAb A6B8.

Histologic Analysis. Hematoxylin and eosin staining of serially sectioned early embryos was performed as described by Kaufman (22). "Normal" vs. "mutant" appearance of each embryo was scored blindly by two independent investigators, based on the known gross appearance of nullizygous mutants at these time points, with 100% concurrence. Apoptotic cells were identified by terminal deoxynucleotidyltransferase-mediated UTP end-labeling assay as described (23). For proliferative assessment of embryonic tissues, BrdUrd staining was performed as described (24), using a BrdUrd staining kit (Oncogene Research).

***In Vitro* Culture and Radiation Treatment of Blastocysts.** Blastocysts were isolated at embryonic day 3.5 (E3.5) from intercrosses between *mrad50*Brdm1 heterozygotes and then cultured in M15 for 6 days as described (25). For radiation treatment, blastocysts were exposed to 2 Gy of γ-radiation in a Gammacell 1000 irradiator (1 Gy/min) before plating.

PCR Genotyping. A three-primer PCR strategy was used to simultaneously amplify target sequences from both the wild-type and the mutant *mRad50* alleles. A shared primer (*3Rad50t1*: 5′-gtc tgc tac ctt ccg gaa cta-3′) was designed according to the sequence of intron 1 of the *mRad50* gene, 120 bp downstream from the deletion junction of the second
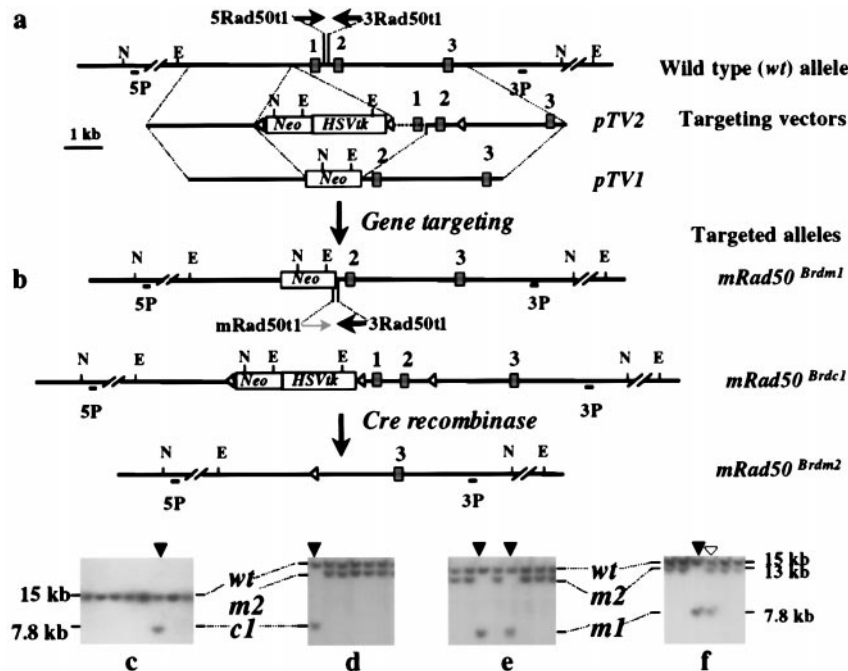

Fig. 1. Gene targeting at the *mRad50* locus. (*a*) Structure of the *mRad50* locus and targeting vectors *pTV1* and *pTV2*. The Southern blot hybridization analysis strategy was the same for the identification of targeted events generated by both targeting vectors. (*b*) Targeted clones first were identified by using a 5′ external probe (5P), which detects the change of a 15-kb wild-type *Nco*I fragment to a novel 7.8-kb *Nco*I fragment, and then were confirmed with a 3′ external probe (3P), which detects the change of a 17-kb wild-type *Eco*RV fragment into a novel 14-kb *Eco*RV fragment. The targeted allele generated by *pTV1* is a null allele (designated *mrad50*Brdm1 or *m1*). The targeted allele using *pTV2* as a vector is a conditional null allele (*mrad50*Brdc1 or *c1*). Cre recombinase-mediated removal of the *PGK-neo/HSVtk* cassette plus exons 1 and 2 of the *mRad50* allele results in a null allele (the *mrad50*Brdm2 or *m2* allele), changing the 7.8-kb *mrad50*Brdc1 allele *Nco*I fragment into a 13-kb *Nco*I fragment. The primers indicated by arrows enable PCR identification of the wild-type (5Rad50t1 + 3Rad50t1) and *mrad50*Brdm1 alleles (mRad50t1 + 3Rad50t1). (*c*) Identification of a targeted clone from the *pTV2* targeting vector. A targeted event is indicated by an arrow. The 15-kb *Nco*I fragment of the wild-type (*wt*) allele and the 7.8-kb fragment of the primary targeted (*c1*) allele are indicated. (*d*) Removal of the *PGK-neo/HSVtk* cassette plus exons 1 and 2 of *mRad50* from the *c1* allele by Cre to generate the *m2* allele. The parental cell line is indicated by an arrow. The 13-kb *Nco*I fragment of the *m2* allele is also indicated. (*e*) Gene targeting in *mRad50*/*mrad50*Brdm2 ES cells with *pTV1*. Two clones in which the *m2* mutant allele was retargeted to generate a null allele, *mrad50*Brdm1 (*m1*), are indicated (arrows). (*f*) Gene targeting with *pTV1* in trisomic chromosome 11 mutant ES cells that contain two copies of the *wt* allele and one copy of the *m2* allele. Retargeting of the mutant allele is indicated by an arrow whereas targeting of one of two *wt* alleles is indicated by an open arrowhead.

Table 1.   Gene targeting at the *mRad50* locus

Cell line (genotype)	Targeting vector	No. of colonies analyzed	No. targeted to wt allele*	No. targeted to mutant allele*
AB2 (+/+)	*pTV2*	159	20 (6.3%)	NA
AB2 (+/+)	*pTV1*	86	8 (4.7%)	NA
M2-1 (+/*m2*)	*pTV1*	146	0	6 (4.1%)
M2-2 (+/+/*m2*)	*pTV1*	92	7 (3.8%)	7 (7.6%)

NA, not applicable. wt, wild type.
*Targeting frequency per locus in parentheses.

targeting vector (Fig. 1*a*). This primer can pair with a wild-type, allele-specific primer (*5Rad50t1*: 5′-cca gaa ggt gtt tag ggc gt-3′) within the deleted region to amplify a 170-bp product from the wild-type allele or with a targeted allele-specific primer (*mRad50t1*: 5′-cct agc cgc ttc cat tgc tca-3′) within the PGK promoter in the *neo* cassette to amplify a 350-bp product from the mutant allele. PCR products were resolved on 2% agarose gels (Fig. 4*e*). The recovery of cells and DNA isolation from blastocyst explants for genotyping has been described (25).

RESULTS AND DISCUSSION

***mRad50* Is Essential for Cellular Viability.** To define the function of the mammalian homologue of *Rad50*, we generated mutant alleles of *mRad50* by using ES cell technology. Two replacement targeting vectors were designed to generate a mutation in the *mRad50* locus by deleting the highly conserved ATP-binding motif present in exon 1 (Fig. 1*a*). Mutation of this region in *ScRAD50* confers a null phenotype (26). *pTV1* was designed to delete exon 1 and replace it with a *PGK-neo* selection cassette, generating a null allele (*mrad50*[Brdm1], abbreviated as *m1*). *pTV2* was designed to generate a conditional null allele (*mrad50*[Brdc1], abbreviated as *c1*). In this vector, a *neo-HSVtk* cassette flanked by two *loxP* sites was inserted upstream of exon 1 and a third *loxP* site was positioned in intron 2. Cre recombinase mediates a recombinational event between paired *loxP* recognition sites, with resultant deletion of intervening sequence. The conditional allele *c1* therefore can be converted into a null allele (*mrad50*[Brdm2], abbreviated as *m2*) by expression of Cre. The recombinational event between the first and third *loxP* sites results in the deletion of exons 1 and 2 along with the selection marker cassette, allowing 1-(2-deoxy-2-fluoro-β-D-arabinofuranosyl)-5-iodouracil-negative selection for clones in which this event has taken place. *pTV1* and *pTV2* were transfected into ES cells to generate targeted clones, which were identified by Southern blotting using the enzymes and probes detailed in Fig. 1.
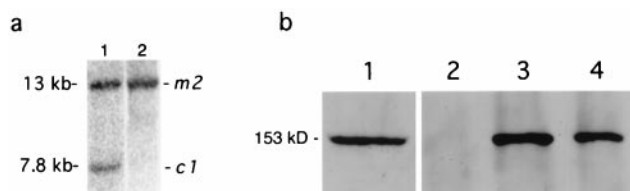

FIG. 2.   Creation of nullizygous cells in the presence of *pmRad50* expression plasmid. (*a*) Southern blot of *Nco*I-digested DNA from *m2/c1* cells before (lane 1) and after (lane 2) Cre-mediated recombination event deleting exons 1 and 2 in the presence of *pmRad50*. External probe 5P hybridizes to a 13-kb *m2*-specific fragment and a 7.8-kb *c1*-specific fragment. (*b*) *mRad50* expression in cDNA-complemented *m2/m2* cell lines. Fractionated extracts of wild-type (lanes 1–3) or *m2/m2* complemented with *pmRad50* (lane 4) cells, immunoblotted with mRad50 mAb. Wild-type whole-cell extract (lane 1); wild-type cell extracts immunoprecipitated with preimmune serum (lane 2) or mMre11 antiserum (lane 3); and *m2/m2/pmRad50* cell extract immunoprecipitated with mMre11 antiserum (lane 4).

Immunoprecipitation and immunoblot analysis demonstrated that the mMre11/mRad50 complex was present in ES cells (data not shown). We therefore attempted to establish mRad50 deficiency in that context. Whereas heterozygous +/*m1* and +/*m2* mutant ES cells had grossly normal proliferative capacity (with plating efficiencies and doubling times similar to those of wild-type parental cell lines), two approaches to derive null (*m1/m2* or *m2/m2*) ES cells were unsuccessful. First, ES cells with the +/*m2* genotype were retransfected with the *pTV1* targeting vector. Although six independent targeting events were identified, all were retargeted at the *mrad50*[Brdm2] allele (Table 1; Fig. 1*e*). In contrast, targeting of the wild-type locus in an ES cell line with one *m2* allele and two wild-type alleles (caused by trisomy 11) was successful (Table 1; Fig. 1*f*). Second, compound heterozygous ES cells with the *m2/c1* genotype could not be converted into the *m2/m2* genotype by transient expression of Cre. The recombinase was clearly functional in these experiments, because Southern analysis of 225 clones revealed that all had deleted the selection markers flanked by *loxP* sites. However, no clones with exons 1 and 2 deleted were recovered. Ectopic expression of mRad50 in these *m2/c1* cells from the wild-type cDNA expression vector *pmRad50* allowed conversion of *m2/c1* clones into the *m2/m2* genotype (Fig. 2*a*). In these nullizygous clones, reverse transcription–PCR analysis using a silent mutation engineered into *TV2* demonstrated expression only from the wild-type *pmRad50* cDNA (data not shown), and immunoprecipitation/immunoblot analysis confirmed the presence of wild-type mRad50 in the mMre11/mRad50 protein complex (Fig. 2*b*). Thus, mRad50 appears to be essential for ES cell viability, as has been demonstrated for mMre11 (27).

***mRad50* Deficiency Causes Early Embryonic Death.** To delineate further the function of mRad50, the *mrad50*[Brdm1] allele was established in the mouse germ line by using standard procedures. Heterozygous (+/*m1*) mice were indistinguishable from their wild-type littermates in viability, growth, development, and fertility. Pairs of heterozygous mutant mice were intercrossed to generate homozygous mutants (*m1/m1*), but genotype analysis at term failed to identify any animals of this genotype (*n* = 205), whereas +/+ and +/*m1* mice were recovered in a 1:2 ratio.

To investigate the cause of embryonic lethality, timed matings were set up and embryos were recovered between E5.5 and E8.5. Of 17 embryos dissected from their decidua between E7.5 and E8.5, 5 were significantly smaller than their littermates, including two that were largely resorbed. The 3 "abnormal" nonresorbed embryos were confirmed to be homozygous mutants by PCR whereas none of the "normal" embryos were homozygotes. To obtain further insight into the nature of the developmental defects in the *m1/m1* mutants, embryos were collected in their decidua between E5.5 and E7.5 and sectioned serially (Fig. 3). Morphologic abnormalities could not be discerned in any of 18 E5.5 embryos examined. At E6.0, 3 of 14 embryos were overtly smaller than their littermates. In these smaller embryos, the endodermal and ectodermal cells were packed loosely and appeared not to form the normal columnar ectoderm (Fig. 3 *a* and *b*). At E6.5, 3 of 16 embryos examined also were abnormal (Fig. 3 *c* and *d*). Although
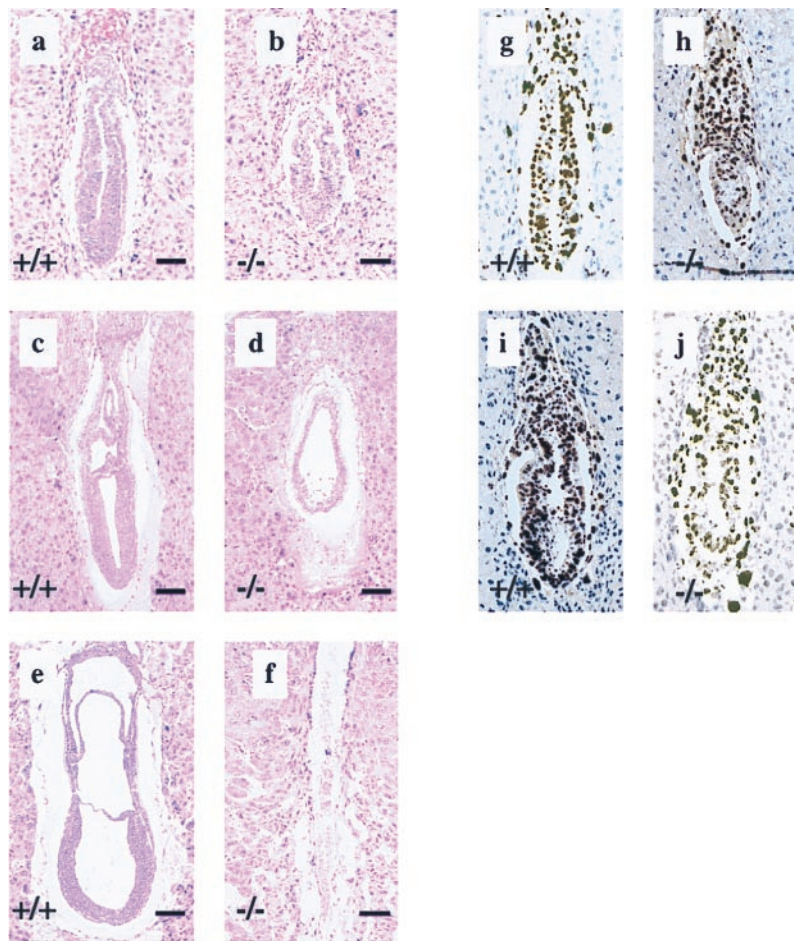
FIG. 3.   Development of *mrad50* mutant embryos. (*a–f*) Hematoxylin/eosin staining of sagittal sections of wild-type embryos (*a, c,* and *e*) and mutant embryos (*b, d,* and *f*) at E6.0 (*a* and *b*), E6.5 (*c* and *d*), and E7.5 (*e* and *f*). Note the smaller size of the mutant embryos. By E6.5, the homozygous mutant embryo has not developed appreciably beyond E6.0 stage. In many cases, the mutant embryo is in the process of being resorbed. By E7.5, the homozygous mutant embryo is completely resorbed. (Bar = 100 μm.) (*g–j*) BrdUrd labeling of proliferating cells in wild-type (*g* and *i*) and mutant (*h* and *j*) embryos at E6.0 and E6.5, respectively.

embryonic tissues were still recognizable, they had not developed appreciably, resembling E6.0 embryos both in size and degree of germ-layer differentiation. Some embryos were being resorbed (Fig. 3*d*). At E7.5, 4 of 15 embryos examined were in advanced stages of resorption (Fig. 3 *e* and *f*). Based on an expected frequency of 25% mutant embryos from these crosses, these studies suggest that the *m1/m1* embryos become abnormal by E6.0 and are largely resorbed by E7.5.

The mechanism of embryonic death was examined by BrdUrd incorporation assays in parallel with terminal deoxynucleotidyltransferase-mediated UTP end-labeling analyses of embryos arising from timed matings. One-half of the litters were labeled *in utero* with BrdUrd for 2 hr before harvest, and BrdUrd incorporation was examined immunohistochemically (24); the other half were sectioned and labeled with terminal deoxynucleotidyltransferase (TdT) (23). Homozygous mutant embryos were identified by their histologic appearance. TdT-labeled sections from E6.5 embryos showed indistinguishable levels of apoptotic nuclei in normal- and mutant-appearing embryos (data not shown). However, by E6.5, mutant-appearing embryos had fewer BrdUrd-labeled nuclei, suggesting a decrease in the number of proliferating cells (Fig. 3 *h* and *j*). Taken together, these data suggest that the developmental abnormality in mutant embryos does not arise from high levels of apoptosis, but instead may be a result of decremental cessation of proliferation.

mRad50-Deficient Cells Are Radiosensitive. The early embryonic death of *m1/m1* mutants precluded a detailed analysis of DSB repair. Because the *m1/m1* mutants survived *in vivo* until E6.0, the functional relevance of *mRad50* in DSB repair was examined *in vitro* by using explanted blastocysts. In this assay, blastocysts isolated at E3.5 from +/*m1* females crossed with +/*m1* males were γ-irradiated and placed into culture. After 6 days, the embryos were examined and then genotyped. The giant trophoblast and inner cell mass components of the mRad50-deficient blastocysts (*m1/m1*) developed normally in unirradiated controls (Fig. 4 *a* and *c*). After γ-irradiation (2 Gy), all *m1/m1* embryo outgrowths ($n = 10$) had lost their inner cell masses and only the nonmitotic trophoblast giant cells remained viable (Fig. 4*d*), whereas all +/+ ($n = 9$) and +/*m1* ($n = 21$) embryos proliferated normally (Fig. 4*b*), apparently unaffected by the γ-irradiation. Embryo genotypes were confirmed by PCR (Fig. 4*e*). These data demonstrate that mRad50 deficiency leads to differential radiation sensitivity in the blastocyst explants. The mitotically active diploid embryonic ectoderm cells of the embryo are ablated by 2 Gy of γ-irradiation, whereas the nonmitotic trophoblast giant cells with endoreduplicated DNA appear unaffected. Thus, *mRad50* functions in the DNA-damage response of murine cells, as predicted from the phenotypic features of *Scrad50* mutant strains.

The Essential Functions of mRad50. The DSB recognition and signaling functions of the mammalian Mre11/Rad50 protein complex are not essential, as they are abrogated in Nijmegen breakage syndrome cells (14, 28). Similarly, it is unlikely that the presumptive nonhomologous end joining
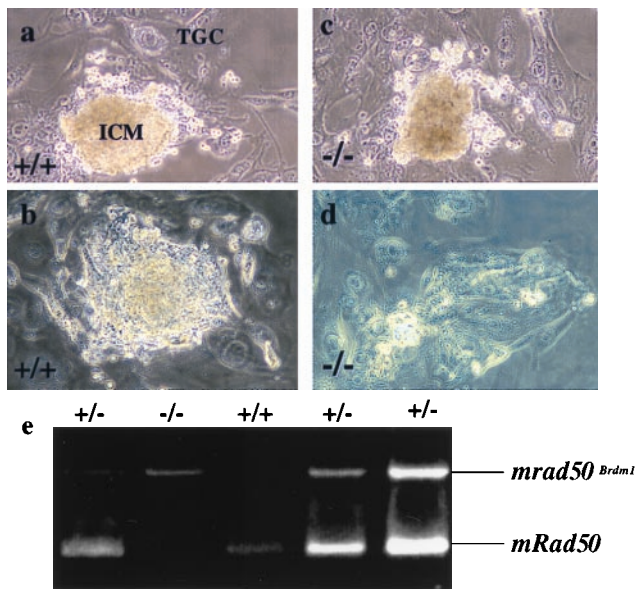
FIG. 4. *In vitro* culture of blastocysts. (*a* and *c*) Blastocyst explants after 6 days without radiation treatment. Proliferation of both the inner cell mass (ICM) and the trophoblast giant cells (TGC) is prominent in both the wild-type (*a*) and mutant (*c*) embryos. (*b* and *d*) Blastocyst explants 6 days after 2 Gy γ-irradiation. Notice the active proliferation of both the inner cell mass and the trophoblast cells in the wild-type embryo (*b*). In contrast, in the mutant embryo, the inner cell mass is completely ablated (*d*). (*e*) Typical PCR genotyping of the blastocyst explants at the end of the experiment.

functions of this complex are essential, because disruption of the DNA end-joining pathway via mutations in the DNA-PK complex (29–32), DNA ligase IV (33), or XRCC4 (34) is not lethal, suggesting that this pathway is nonessential.

The data presented here are compatible with a synergistic effect of disrupting both the presumptive DSB recognition/signaling and DNA end-joining functions of the murine Mre11/Rad50 protein complex, leading to progressive failure of cell growth. However, an alternative hypothesis is supported by the observation that *Scmre11*, *Scrad50*, and *xrs2* mutant strains are impaired in their ability to use the sister chromatid for DSB repair, suggesting that the Mre11/Rad50 complex is required for the establishment or maintenance of sister chromatid interactions (D. Bressan, B. K. Baxter, and J.H.J.P., unpublished data) (7, 35, 36). *mrad50*[Brdm1]/*mrad50*[Brdm1] embryos reach the early primitive streak stage, indicating that limited cell proliferation can occur in the absence of mRad50. The appearance of the histologic abnormalities in *mrad50*[Brdm1]/*mrad50*[Brdm1] embryos coincides with a period of embryonic development during which proliferation increases dramatically, with estimated mean cell cycle times in the epiblast decreasing from 11.5 hr between E5.5 and 6 down to 4.4 hr between E6.5 and E7 (37). The bulk of spontaneously occurring DSBs is likely to arise during DNA replication, and available evidence suggests that such breaks are repaired primarily through homologous recombination with the sister chromatid (38, 39). The death of *mrad50*[Brdm1]/*mrad50*[Brdm1] cells at E6.5, when rapid proliferation normally occurs, may reflect that sister chromatid-based repair of such spontaneously arising DSBs is abrogated in the absence of mRad50.

In this scenario, decremental failure of proliferating cells could be attributed to the accumulation of unrepaired or misrepaired spontaneous DSBs over several cell cycles. Experiments using a conditional *Gdmre11* mutant in the DT40 chicken cell line support this hypothesis. After inactivation of the *GdMRE11* gene, these cells proceed through several cell cycles before death. Karyotypic analysis during this process reveals that chromosomal aberrations begin to accumulate by

72 hr after Mre11 depletion (Y. Yamaguchi-Iwai and S. Takeda, personal communication).

Interestingly, analysis of conditional *rad51* mutant cells similarly has implicated that protein in the resolution of spontaneous DSBs generated during DNA replication (40). mRad51 deficiency results in lethality by a failure of cell proliferation analogous to that caused by mRad50 deficiency (25, 41, 42). These data argue that homologous recombination is linked to cellular proliferation and that this link is responsible for the failure of *mrad50* cells to meet the intense replicative demand of early embryogenesis.

1. Kanaar, R. & Hoeijmakers, J. H. J. (1997) *Genes Funct.* **1**, 165–174.
2. Petrini, J. H., Bressan, D. A. & Yao, M. S. (1997) *Semin. Immunol.* **9**, 181–188.
3. Haber, J. E. (1998) *Cell* **95**, 583–586.
4. Tsukamoto, Y., Kato, J. & Ikeda, H. (1996) *Genetics* **142**, 383–391.
5. Milne, G. T., Jin, S., Shannon, K. B. & Weaver, D. T. (1996) *Mol. Cell. Biol.* **16**, 4189–4198.
6. Boulton, S. J. & Jackson, S. P. (1996) *EMBO J.* **15**, 5093–5103.
7. Moore, J. K. & Haber, J. E. (1996) *Mol. Cell. Biol.* **16**, 2164–2173.
8. Roeder, G. S. (1997) *Genes Dev.* **11**, 2600–2621.
9. Lee, S. E., Moore, J. K., Holmes, A., Umezu, K., Kolodner, R. D. & Haber, J. E. (1998) *Cell* **94**, 399–409.
10. Kironmai, K. M. & Muniyappa, K. (1997) *Genes Cells* **2**, 443–455.
11. Nelms, B. E., Maser, R. S., MacKay, J. F., Lagally, M. G. & Petrini, J. H. J. (1998) *Science* **280**, 590–592.
12. Nove, J., Little, J. B., Mayer, P. J., Troilo, P. & Nichols, W. W. (1986) *Mutat. Res.* **163**, 255–262.
13. Paull, T. T. & Gellert, M. (1998) *Mol. Cell* **1**, 969–979.
14. Carney, J. P., Maser, R. S., Olivares, H., Davis, E. M., Le Beau, M., Yates, J. R., III, Hays, L., Morgan, W. F. & Petrini, J. H. J. (1998) *Cell* **93**, 477–486.
15. Varon, R., Vissinga, C., Platzer, M., Cerosaletti, K. M., Chrzanowska, K. H., Saar, K., Beckmann, G., Seemanova, E., Cooper, P. R., Nowak, N. J., *et al.* (1998) *Cell* **93**, 467–476.
16. Soriano, P., Montgomery, C., Geske, R. & Bradley, A. (1991) *Cell* **64**, 693–702.
17. Petrini, J. H. J., Xiao, Y.-H. & Weaver, D. T. (1995) *Mol. Cell. Biol.* **15**, 4304–4308.
18. Ramirez-Solis, R., Liu, P. & Bradley, A. (1995) *Nature (London)* **378**, 720–724.
19. McMahon, A. P. & Bradley, A. (1990) *Cell* **62**, 1073–1085.
20. Ramirez-Solis, R., Rivera-Perez, J., Wallace, J. D., Wims, M., Zheng, H. & Bradley, A. (1992) *Anal. Biochem.* **201**, 331–335.
21. Dolganov, G. M., Maser, R. S., Novikov, A., Tosto, L., Chong, S., Bressan, D. A. & Petrini, J. H. J. (1996) *Mol. Cell. Biol.* **16**, 4832–4841.
22. Kaufman, M. H. (1992) *The Atlas of Mouse Development* (Academic, London).
23. Gavrieli, Y., Sherman, Y. & Ben-Sasson, S. A. (1992) *J. Cell Biol.* **119**, 493–501.
24. Hayashi, Y., Koike, M., Matsutani, M. & Hoshino, T. (1988) *J. Histochem. Cytochem.* **36**, 511–514.
25. Sharan, S. K., Morimatsu, M., Albrecht, U., Lim, D. S., Regel, E., Dinh, C., Sands, A., Eichele, G., Hasty, P. & Bradley, A. (1997) *Nature (London)* **386**, 804–810.
26. Alani, E., Padmore, R. & Kleckner, N. (1990) *Cell* **61**, 419–436.

27. Xiao, Y. & Weaver, D. T. (1997) *Nucleic Acids Res.* **25,** 2985–2991.
28. Shiloh, Y. (1997) *Annu. Rev. Genet.* **31,** 635–662.
29. Nussenzweig, A., Chen, C., da Costa Soares, V., Sanchez, M., Sokol, K., Nussenzweig, M. C. & Li, G. C. (1996) *Nature (London)* **382,** 551–555.
30. Taccioli, G. E., Gottlieb, T. M., Blunt, T., Priestley, A., Demengeot, J., Mizuta, R., Lehmann, A. R., Alt, F. W., Jackson, S. P. & Jeggo, P. A. (1994) *Science* **265,** 1442–1445.
31. Blunt, T., Finnie, N. J., Taccioli, G. E., Smith, G. C., Demengeot, J., Gottlieb, T. M., Mizuta, R., Varghese, A. J., Alt, F. W., Jeggo, P. A. & Jackson, S. P. (1995) *Cell* **80,** 813–823.
32. Kirchgessner, C. U., Patil, C. K., Evans, J. W., Cuomo, C. A., Fried, L. M., Carter, T., Oettinger, M. A. & Brown, J. M. (1995) *Science* **267,** 1178–1183.
33. Grawunder, U., Zimmer, D., Fugmann, S., Schwarz, K. & Lieber, M. R. (1998) *Mol. Cell* **2,** 477–484.
34. Li, Z., Otevrel, T., Gao, Y., Cheng, H.-L., Seed, B., Stamato, T. D., Taccioli, G. E. & Alt, F. W. (1995) *Cell* **83,** 1079–1089.
35. Ivanov, E. L., Korolev, V. G. & Fabre, F. (1992) *Genetics* **132,** 651–664.
36. Fabre, F., Boulet, A. & Roman, H. (1984) *Mol. Gen. Genet.* **195,** 139–143.
37. Hogan, B. (1994) *Manipulating the Mouse Embryo: A Laboratory Manual* (Cold Spring Harbor Lab. Press, Plainview, NY).
38. Leach, D. R. (1994) *BioEssays* **16,** 893–900.
39. Cox, M. M. (1998) *Genes Cells* **3,** 65–78.
40. Sonoda, E., Sasaki, M. S., Buerstedde, J. M., Bezzubova, O., Shinohara, A., Ogawa, H., Takata, M., Yamaguchi-Iwai, Y. & Takeda, S. (1998) *EMBO J.* **17,** 598–608.
41. Lim, D. S. & Hasty, P. (1996) *Mol. Cell. Biol.* **16,** 7133–7143.
42. Tsuzuki, T., Fujii, Y., Sakumi, K., Tominaga, Y., Nakao, K., Sekiguchi, M., Matsushiro, A., Yoshimura, Y. & Morita, T. (1996) *Proc. Natl. Acad. Sci. USA* **93,** 6236–6240.